Journal of Sustainable Development of Energy, Water and Environment Systems

http://www.sdewes.org/jsdewes

Year 2025, Volume 13, Issue 2, 1130553

Original Research Article

An Enforcing Resilience of Steep-slope Citrus Orchards against Slope Failure Caused by Torrential Rain

***Tomoki Izumi*[*1], *Naoyuki Yamashita*[2], *Noriyuki Kobayashi*[3]**

[1]Graduate School of Agriculture, Ehime University, 3-5-7 Tarumi, Matsuyama, Ehime, Japan
e-mail: izumi.tomoki.mm@ehime-u.ac.jp

[2]Graduate School of Agriculture, Ehime University, 3-5-7 Tarumi, Matsuyama, Ehime, Japan
e-mail: yamashita.naoyuki.kt@ehime-u.ac.jp

[3]Graduate School of Agriculture, Ehime University, 3-5-7 Tarumi, Matsuyama, Ehime, Japan
e-mail: kobayashi.noriyuki.mu@ehime-u.ac.jp

Cite as: Izumi, T., Yamashita, N., Kobayashi, N., An Enforcing Resilience of Steep-slope Citrus Orchards against Slope Failure Caused by Torrential Rain, J.sustain. dev. energy water environ. syst., 13(2), 1130553, 2025, DOI: https://doi.org/10.13044/j.sdewes.d13.0553

ABSTRACT

In Japan, citrus orchards have traditionally been located on steep slopes because of their favourable growing conditions. However, the unexpected torrential rain that hit western Japan in 2018 caused numerous slope failures in these steep-slope citrus orchards. This study aims to investigate a method to enforce the resilience of steep-slope citrus orchards against torrential rain-induced slope failures by changing the surface soil permeability in such orchards. Laboratory-scale rainfall infiltration experiments were conducted using soil tanks with different surface soil permeabilities by mixing clay. The results demonstrated that the higher the clay mixing ratio, the more rainfall infiltration was suppressed, thereby reducing the slope safety factor decrease. Therefore, it can be concluded that this method is effective for slope stability. However, achieving optimal permeability to stabilise the slope and provide the required water remains a challenge for the future, as it is necessary to provide the water needed for citrus cultivation.

KEYWORDS

Soil improvement, Citrus orchard, Steep slope, Torrential rain, Slope failure, Rainfall infiltration experiment, Slope stability.

INTRODUCTION

There has been a growing interest in infrastructure resilience to achieve a sustainable society in recent years. For instance, a study on the resilience of road infrastructure argues the importance of digital engineering for resilient infrastructure outcomes [1]. Another study has looked at resilient urban water systems to meet energy generation and new water demands in growing cities [2]. In addition, a study has proposed methodologies to assess energy resilience and security and analyze energy sustainability and risks in megacities [3]. A study has also proposed a risk assessment method in green construction using resilience engineering techniques based on functional resonance analysis and analytic hierarchy process methodologies [4]. Furthermore, defining the resilience capacities as absorptive, adaptive, and recovery/restorative capacity, a resilience analysis framework and a metric for measuring

* Corresponding author

resilience have been proposed [5]. In the field of agriculture, a study reviewed the evidence on the potential for integrating agricultural systems, which are defined as collections of agricultural activities, to increase resilience to climate change [6]. A framework to assess the resilience of farming systems and a methodology to operationalize its framework has also been proposed [7]. However, there are few studies related to the resilience of agricultural infrastructure such as farmland, reservoirs, and irrigation/drainage canals. As the ninth goal of the SDGs is to build resilient infrastructure, it is also essential to enhance the resilience of agricultural infrastructure.

Japan is susceptible to natural disasters such as earthquakes, tsunamis, typhoons, torrential rains, and heavy snowfalls due to geographical, topographical, and climatic conditions. These disasters have become more severe and frequent in recent years due to climate change [8]. The Japanese government recognises that preparing for large-scale natural disasters in advance from ordinary times is crucial to avoid repeating post-disaster measures that can take a long time to recover and reconstruct. To achieve this, the government is promoting initiatives for building "National resilience" to proactively prevent and mitigate disasters, and rapidly recover and reconstruct [9]. This study addresses the development of a method to enhance the strength of agricultural land infrastructure as part of the National resilience.

Citrus cultivation in Japan has used steep mountain slopes as citrus orchards because of their excellent growing conditions, such as good sunlight and drainage. In Ehime Prefecture, one of Japan's major citrus production areas, 44% of the citrus orchards are located on steep slopes of more than 15 degrees [10]. However, the unexpected torrential rain that hit western Japan from June 28th to July 8th, 2018, caused numerous slope failures in such steeply sloping orchards, and the citrus industry in Ehime Prefecture suffered tremendous damage.

The Japan Meteorological Agency (JMA) named the torrential rain "The heavy rain event of July 2018" due to the significant damage it caused. The torrential rain brought record-breaking precipitation over western Japan, including Ehime Prefecture and the Tokai region, over a long period. The total rainfall exceeded 1,800 mm in some stations of the JMA Automated Weather Data Acquisition System (AMeDAS) in the Shikoku region and 1,200 mm in the Tokai region, recording two to four times the average monthly precipitation in July for ten days. In addition, the largest 24-hour, 48-hour, and 72-hour precipitations in recorded history were observed at many AMeDAS stations [11]. It has also been pointed out as a characteristic of the torrential rain that many line-shaped precipitation systems formed in a back-building manner, and areas affected by line-shaped precipitation systems experienced locally concentrated heavy rainfall for long periods [12]. Izumi *et al*. noted from July 5 to 8 precipitation records at AMeDAS stations in Ehime Prefecture that in addition to a multimodal precipitation pattern, the return period of peak hourly precipitation was 3 to 25 years, indicating that a considerable amount of rainfall occurred in a very short time [13]. They also obtained the Soil Water Index (SWI) [14], a criterion for meteorological warnings and landslide alerts. Then, they reported that many locations exceeded the emergency warning, a highly unusual phenomenon that occurs once every few decades based on a 50-year probability [13].

This unprecedented torrential rain caused numerous slope failures in Ehime Prefecture. Mori and Ono reported 883 new cases [15] in addition to the 413 landslide records already documented [16]. They also calculated precipitation thresholds for landslide incidence for each geological belt using the SWI. Their findings revealed that the Shimanto Belt, located in the southern part of Ehime Prefecture, where citrus cultivation is prevalent, has a lower precipitation threshold than other geological belts. Kimura *et al*. investigated the relationship between vegetation and landslides in the Shimanto Belt [17]. They calculated the landslide density and area ratio and found these values were exceptionally high in citrus orchard areas. Ishiguro and Kawase identified 3,410 slope failures from post-disaster aerial photographs covering approximately 1,200 km^2 of southern Ehime Prefecture, as published by the Geospatial Information Authority of Japan [18].

Slope failure caused by heavy rain is generally due to a rapid increase in soil pore water pressure from rainfall infiltration. To prevent this, it is adequate to quickly drain the infiltrated rainfall by ensuring appropriate drainage or to control rainfall infiltration from the soil surface. Citrus orchards on steep slopes have good drainage characteristics, but there has been no previous effort to reclaim citrus orchards for the purpose of controlling rainfall infiltration. Therefore, this study focuses on controlling rainfall infiltration from the soil surface by changing the surface soil permeability. The effectiveness of this method on rainfall infiltration control and slope stability is investigated through laboratory-scale rainfall infiltration experiments using soil tanks with different surface soil permeabilities achieved by mixing clay.

RAINFALL INFILTRATION EXPERIMENT

In this study, laboratory-scale rainfall infiltration experiments using soil tanks are carried out to investigate the stability of slopes with changed surface soil permeability to rainfall. Below is an overview of the experimental setup, soil improvement material, and experimental conditions.

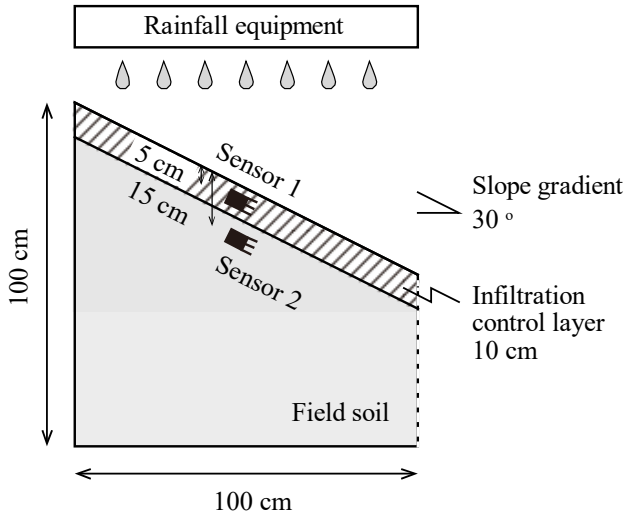

Figure 1. Schematic diagram of the experimental setup

Experimental setup

Figure 1 shows a schematic diagram of the experimental setup. The equipment consists of a 100 cm long × 100 cm wide × 30 cm deep soil tank and rainfall equipment. The front of the soil tank was covered with acrylic panels to observe rainfall infiltration. The metal mesh was also installed at the right end of the soil tank to drain rainfall seepage water. The soil used in the experiment was collected from a citrus orchard located on a steep slope of approximately 30 degrees in Uwajima City, Ehime Prefecture, where a slope failure occurred during the heavy rain event of July 2018 in western Japan. After this, the collected soil is called “field soil.” The field soil was filled into the soil tank so that the slope gradient was 30 degrees, thus reproducing the actual site. The upper 10 cm of the soil tank was set as an infiltration control layer made by mixing the field soil and soil improvement material with low permeability to change surface soil permeability. Dry soil was prepared for both the field soil and the soil improvement material to uniform the initial conditions for the experiment. Two ADR soil moisture sensors (UIZ-SM-2X, UIZIN co., LTD) were installed to obtain time series data of volumetric water content every 30 seconds, as shown in Figure 1. Sensor 1 was embedded at a depth of 5 cm below the soil surface to observe the volumetric water content in the infiltration control layer. Sensor 2 was embedded 15 cm below the soil surface to observe the volumetric water content under the infiltration control layer. In addition, a fixed-point camera (MAC200DN, brinno) was used to capture rainfall infiltration every 30 seconds. The rainfall equipment drips water from nozzles under a constant water level.

Rainfall intensity can be controlled by changing the number and diameter of the nozzles. During the heavy rain event of July 2018, the maximum hourly rainfall at the rainfall observatories in Uwajima City was recorded at 74 to 96 mm/h [19]. The maximum hourly rainfall by the radar/rain gauge analysed precipitation (RRAP) near the soil sampling site was recorded at 105 mm/h [20]. Therefore, this experiment gave 100 mm/h of rainfall intensity to the soil tank for two hours.

Soil improvement material and experimental cases

Kaolin clay, whose chemical formula is $Al_2Si_2O_5(OH)_4$, was employed as the soil improvement material to make it easy to control the permeability of the soil layer. The physical and chemical properties of the field soil and Kaolin clay are summarised in Table 1. Soil particle density and porosity are slightly greater in the Kaolin clay than in the field soil. By three orders, the saturated hydraulic conductivity of the field soil is more significant than that of Kaolin clay. In contrast, the pH values of field soil and kaolin clay are similar (slightly acidic), suggesting that there is little change in the pH of the field soil as a result of mixing the Kaolin clay. The experiment set four cases by mixing the field soil and Kaolin clay ratio, as shown in Table 2. Case 1 is the reference case, which means the case without soil improvement.

Table 1. Physical and chemical properties of the field soil and soil improvement materials

	Field soil	Kaolin clay
Soil particle density [g/cm^3]	2.54	2.64
Porosity [m^3/m^3]	0.400	0.465
Saturated hydraulic conductivity [m/s]	1.05×10^{-4}	4.27×10^{-7}
pH [-]	5.6-5.8	5.8-6.0

Table 2. Experimental cases and mixing ratio of the soil improvement materials

Cases	Mixing ratio [%] Field soil / Kaolin clay
Case 1	100 / 0
Case 2	80 / 20
Case 3	70 / 30
Case 4	50 / 50

RESULTS AND DISCUSSION

This section first discusses the temporal changes in volumetric water content due to rainfall infiltration and then discusses slope safety.

Rainfall infiltration and temporal change of volumetric water content

Figures 2 and 3 show the temporal change of the volumetric water content in Sensors 1 and 2, respectively. From Figure 2, it is found that the time at which the volumetric water content starts to increase tends to be slower as the clay content increases. Table 3 shows the start time of the increase in volumetric water content and the saturated hydraulic conductivity of the infiltration control layer. From Table 3, it is found that the increase in volumetric water content is delayed by the suppression of rainfall infiltration due to the smaller hydraulic

conductivity caused by a larger clay mixing ratio. However, the volumetric water content in Case 2 converges to only 0.21. In contrast, the other cases converge above 0.33, suggesting that in Case 2, the non-uniform flow, like a fingered flow, may be more pronounced than in the other cases. The volumetric water content of Case 4 exhibited an immediate increase at approximately 2,000 s, surpassing the levels observed in the other cases after approximately 3,000 s. This phenomenon is hypothesised to be attributable to selective flow (seepage water infiltrating into larger pore spaces near the sensor) at around 2,000 seconds, along with the slightly higher porosity of the Kaolin clay than that of the field soil. Consequently, the increased clay content reduced hydraulic conductivity and increased seepage pressure, enhancing the propensity for selective flow. It is hypothesised that the volumetric water content exceeded that observed in other cases due to the seepage water flowing into the larger pore in proximity to the sensor. From **Figure 3**, no increase in volumetric moisture content is found except for Case 1, indicating that the rainfall infiltration into the subsurface is suppressed by improving soil permeability. **Figure 4** shows the infiltration after 7,200 seconds (2 hours) captured by the fixed-point camera. The darker colour of the soil indicates the extent of rainfall infiltration. From **Figure 4**, it is found that in the case of the clay mixture, infiltration below the infiltration control layer is almost negligible compared to Case 1, suggesting that vertical infiltration is suppressed and the rainfall flows downward (to the right-hand side of the soil tank) as a slope flow. Especially, in Case 4, no infiltration is observed below the infiltration control layer, suggesting that changing surface soil permeability may impede the growth of citrus trees.

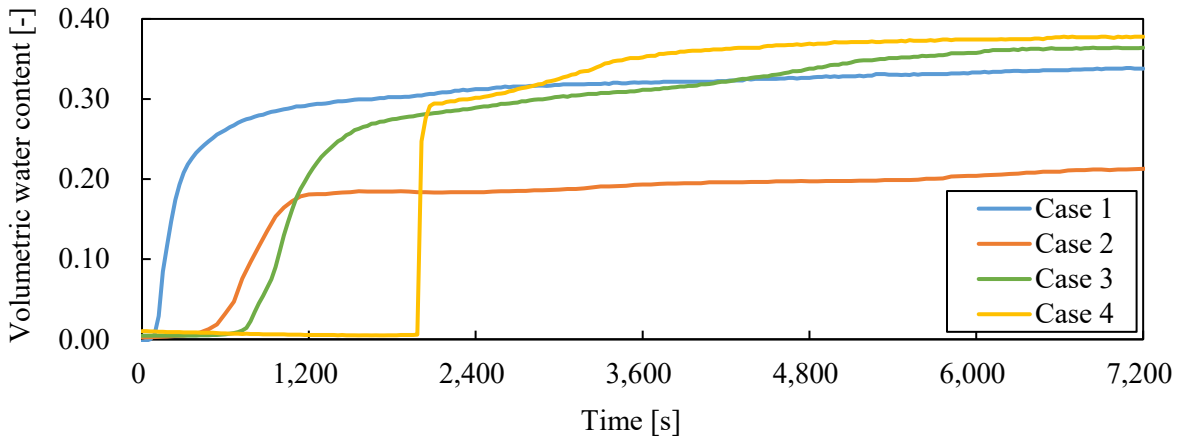

Figure 2. Time-varying volumetric water content in Sensor 1

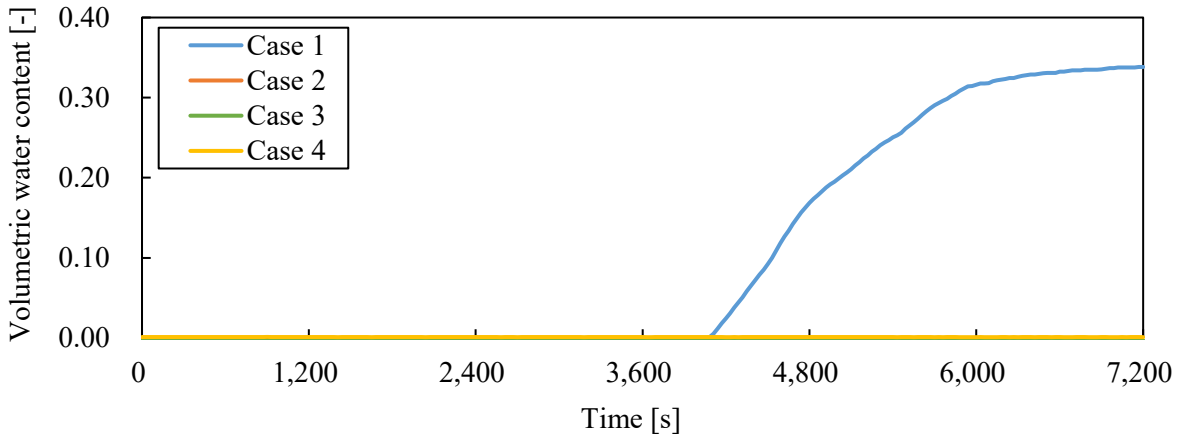

Figure 3. Time-varying volumetric water content in Sensor 2

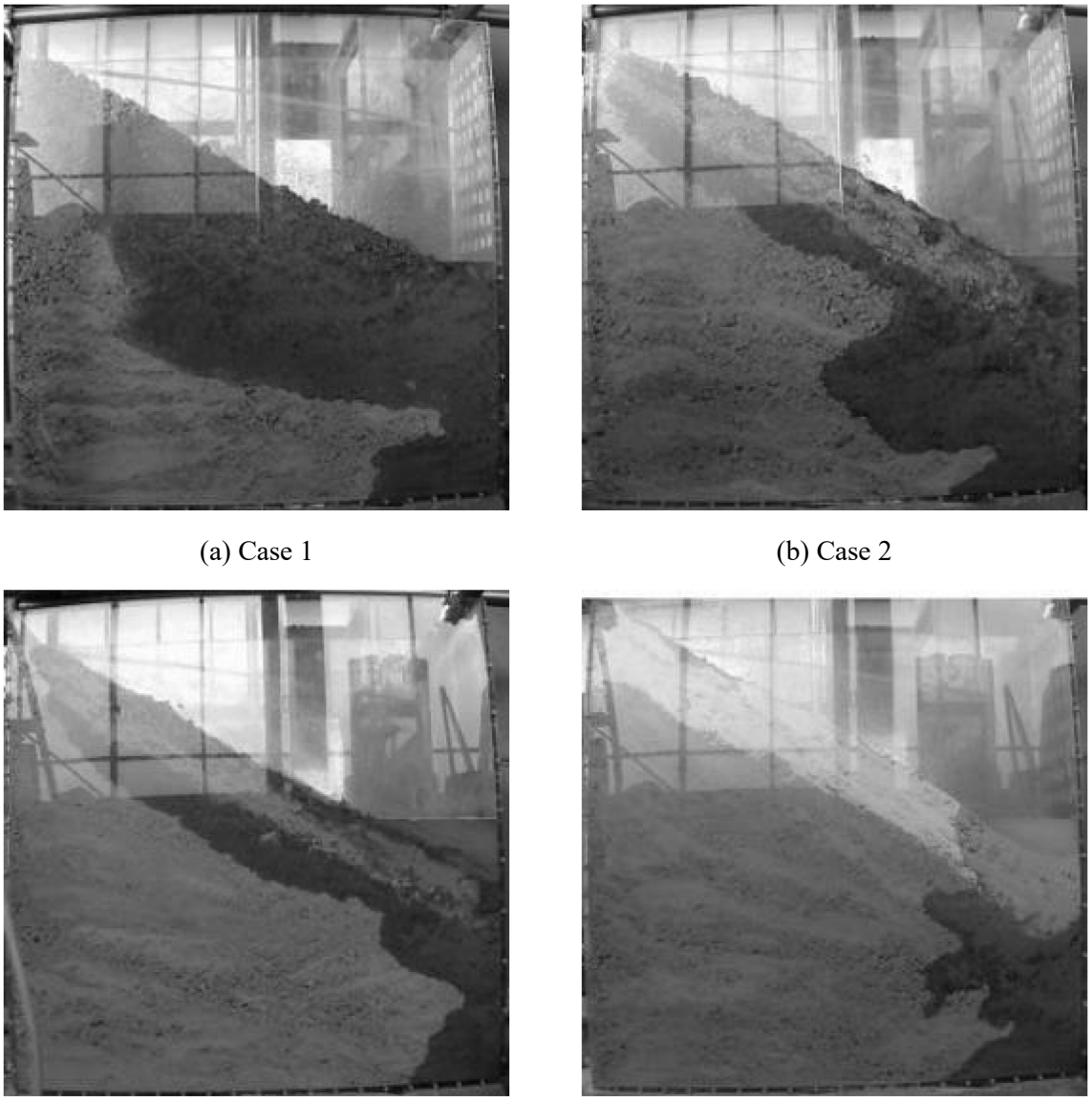

(a) Case 1 (b) Case 2

(c) Case 3 (d) Case 4

Figure 4. Rainfall infiltration 7,200 seconds (2 hours) later

Table 3. The start time of increasing in volumetric water content at Sensor 1 and the saturated hydraulic conductivity in mixing soil layer

	Start time of increasing in volumetric water content [s]	Saturated hydraulic conductivity [m/s]
Case 1	210	3.08×10^{-3}
Case 2	450	1.60×10^{-5}
Case 3	750	6.03×10^{-7}
Case 4	2,160	7.14×10^{-7}

Safety of the slope

Slope stability is discussed for the results of rainfall infiltration experiments. Assuming that the experimental slope is an infinite-length slope, as shown in **Figure 5**, and that the slip surface is parallel to the slope, the slope safety factor F_s can be calculated by the following equations:

$$F_s = \begin{cases} \dfrac{c + \{\gamma_t (Z-H) + \gamma_{sat} H\} \cos^2 \beta \tan \varphi}{\{\gamma_t (Z-H) + \gamma_{sat} H\} \cos \beta \sin \beta} & (Z > H) \\ \dfrac{c + \gamma' Z \cos^2 \beta \tan \varphi}{\gamma_{sat} Z \cos \beta \sin \beta} & (Z \le H) \end{cases} \quad (1)$$

where c is the cohesion [kN/m^2], φ is the angle of shear resistance [degree], γ_t is the wet specific weight [kN/m^3], γ_{sat} is the saturated specific weight [kN/m^3], γ' is the submerged specific weight [kN/m^3], Z is the depth of slip surface [m], H is the infiltration depth [m], β is the slope gradient [degree].

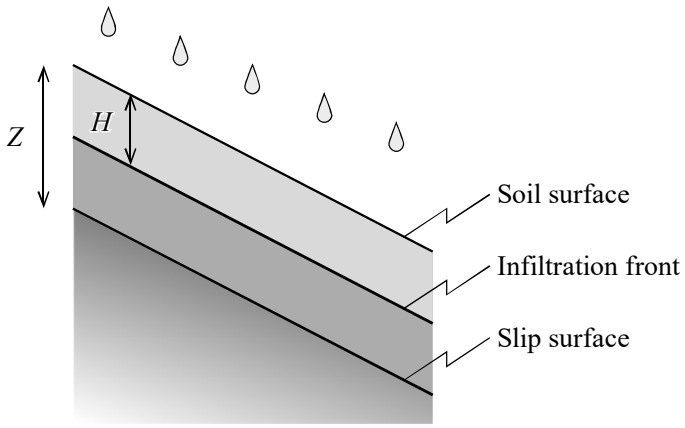

Figure 5. Rainfall infiltration on an infinite-length slope

Figure 6 shows the temporal change of the infiltration depth in each experimental case. **Figure 7** shows the temporal change of the safety factor at Z = 50 cm. From **Figure 6**, it is found that the larger the clay mixing ratio, the smaller the water depth due to rainfall infiltration. In fact, the infiltration depth at 7,200 seconds later was 0.31 m in Case 1, while it was 0.06 m in Case 5. From **Figure 7**, it is found that the slope safety factor decreases with increasing clay mixing ratio due to the suppression of rainfall infiltration. Case 3 had the lowest safety factor at the beginning of the experiment, but the safety factor was slightly decreased with time and then equivalent to that of Case 2 after 7,200 seconds.

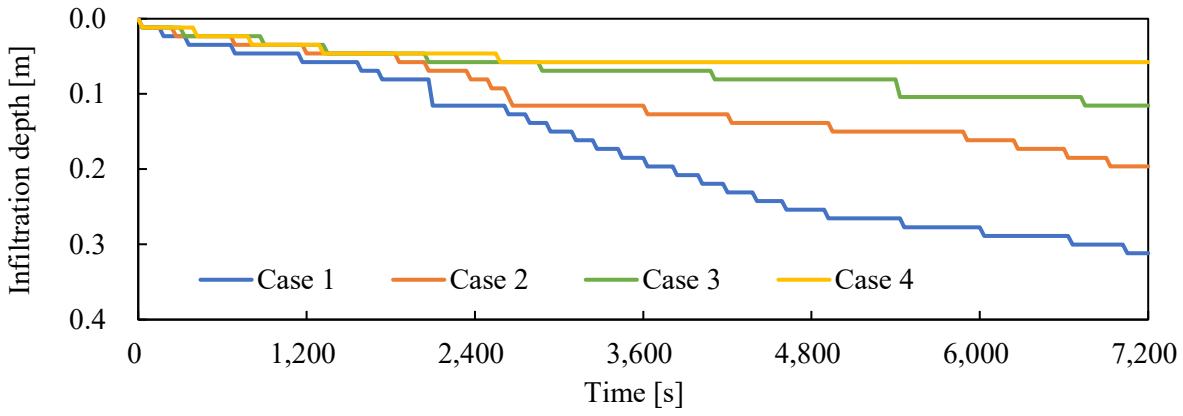

Figure 6. Temporal change of the infiltration depth

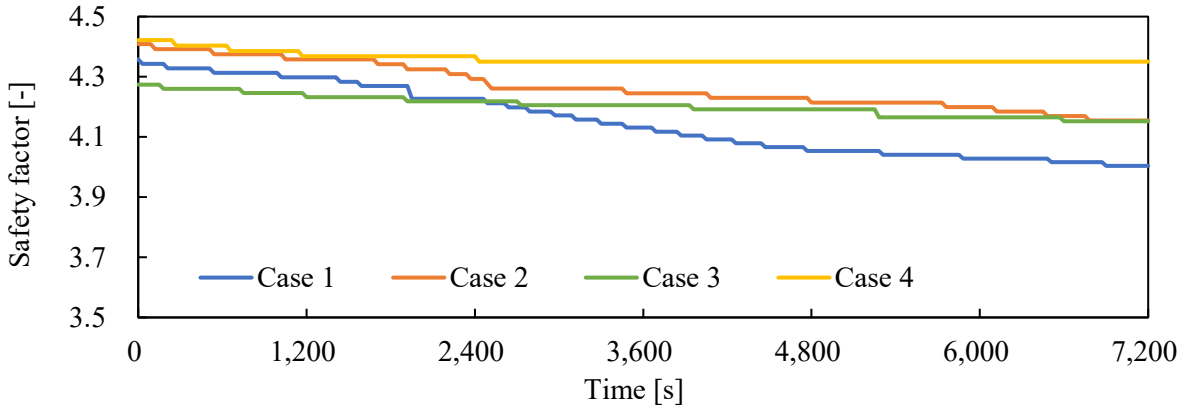

Figure 7. Temporal change of the safety factor at $Z = 50$ cm

Thus, from the perspective of slope stability, lower permeability results in less rainfall infiltration and a more stable slope. Conversely, from the perspective of citrus cultivation, lower permeability results in reduced water availability for citrus growth. One day after the infiltration experiment, the rainfall infiltration below the improved soil layer was observed. It was confirmed that in Cases 1 to 3, the rainfall infiltrated to the bottom of the soil tank. Since the maximum root zone of citrus trees is at most 50 cm, it is considered that the required amount of water could be secured in these cases. Therefore, the results of this experiment suggest that the optimal clay content ratio for both ensuring slope stability and implementing citrus cultivation is between 20% and 50%. However, further study is necessary to determine the appropriate clay mixing ratio to ensure the required amount of water in case of lower rainfall intensity than in this experiment.

CONCLUSIONS

A countermeasure for resilience enhancement that changes permeability by mixing clay with surface soil was studied due to the slope failures in many citrus orchards with steep slopes caused by the heavy rain event of July 2018.

As a result, it was confirmed that the higher the clay mixing ratio, the more rainfall infiltration could be suppressed, thereby reducing the decreasing of the slope safety factor. Therefore, this method effectively enhances steep slopes' resilience against slope failure caused by heavy rainfall. On the other hand, as water is required for citrus cultivation, the clay mixing ratio does not have to be high, suggesting that the optimum clay mixing ratio in this experiment was between 20% and 50%.

Further detailed studies are needed in terms of water requirements for citrus cultivation in the future. The implementation of rainfall infiltration control methodologies at the field scale is also a matter of future concern. However, it is not a viable option to mix clay on the soil surface of the entire citrus orchards. Consequently, numerical analysis could be employed to establish patchy infiltration control layers at locations that significantly contribute to the slope stability of the entire citrus orchards.

ACKNOWLEDGMENTS

This work was supported by JSPS KAKENHI grant number 20H03102 and the Ehime Prefecture Strategic Experiment and Research Project of ‘Project for Technology Development to Support Orchard Disaster Recovery.’

NOMENCLATURE

Symbols

c	cohesion	[kN/m^2]
F_s	safety factor	[-]
H	infiltration depth	[m]
Z	depth of slip surface	[m]

Greek letters

β	slope gradient	[degree]
γ'	submerged specific weight	[kN/m^3]
γ_{sat}	saturated specific weight	[kN/m^3]
γ_t	wet specific weight	[kN/m^3]
φ	angle of shear resistance	[degree]

Subscripts and superscripts

s	safety
sat	saturated
t	wet

Abbreviations

ADR	Amplitude Domain Reflectometry
AMeDAS	Automated Weather Data Acquisition System
JMA	Japan Meteorological Agency
RRAP	Radar/rain gauge analysed precipitation
SDGs	Sustainable Development Goals
SWI	Soil Water Index

REFERENCES

1. S. Caldera, S. Mohamed, S. Mostafa, and C. Desha, ‘Digital engineering for resilient road infrastructure outcomes: Evaluating critical asset information requirements’, J. sustain. dev. energy water environ. syst., vol. 10, no. 1, pp. 1–22, Mar. 2022, https://doi.org/10.13044/j.sdewes.d8.0357.
2. S. H. Sutherland and B. T. Smith, ‘Resilience Implications of Energy Storage in Urban Water Systems’, J. sustain. dev. energy water environ. syst., vol. 6, no. 4, pp. 674–693, Dec. 2018, https://doi.org/10.13044/j.sdewes.d6.0210.
3. G. Mutani and V. Todeschi, ‘Energy Resilience, Vulnerability and Risk in Urban Spaces’, J. sustain. dev. energy water environ. syst., vol. 6, no. 4, pp. 694–709, Dec. 2018, https://doi.org/10.13044/j.sdewes.d6.0203.
4. L. V. Rosa, J. E. M. França, A. N. Haddad, and P. V. R. Carvalho, ‘A Resilience Engineering Approach for Sustainable Safety in Green Construction’, J. sustain. dev. energy water environ. syst., vol. 5, no. 4, pp. 480–495, Dec. 2017, https://doi.org/10.13044/j.sdewes.d5.0174.
5. R. Francis and B. Bekera, ‘A metric and frameworks for resilience analysis of engineered and infrastructure systems’, Reliability Engineering & System Safety, vol. 121, pp. 90–103, Jan. 2014, https://doi.org/10.1016/j.ress.2013.07.004.
6. J. D. B. Gil, A. S. Cohn, J. Duncan, P. Newton, and S. Vermeulen, ‘The resilience of integrated agricultural systems to climate change’, WIREs Climate Change, vol. 8, no. 4, p. e461, Jul. 2017, https://doi.org/10.1002/wcc.461.
7. M. P. M. Meuwissen, P. H. Feindt, A. Spiegel, C. J. A. M. Termeer, E. Mathijs, Y. de Mey, R. Finger, A. Balmann, E. Wauters, J. Urquhart, M. Vigani, K. Zawalińska, H. Herrera, P. Nicholas-Davies, H. Hansson, W. Paas, T. Slijper, I. Coopmans, W. Vroege, A. Ciechomska, F. Accatino, B. Kopainsky, P. M. Poortvliet, J. J. L. Candel, D. Maye, S.

Severini, S. Senni, B. Soriano, C-J. Lagerkvist, M. Peneva, C. Gavrilescu, and P. Reidsma, 'A framework to assess the resilience of farming systems', Agricultural Systems, vol. 176, p. 102656, Nov. 2019, https://doi.org/10.1016/j.agsy.2019.102656.

8. Cabinet Office, Government of Japan, 'White Paper Disaster Management in Japan', 2022. [Accessed: Mar. 09, 2024], Available: https://www.bousai.go.jp/en/documentation/white_paper/pdf/2022/R4_hakusho_english.pdf.
9. Cabinet Secretariat, Government of Japan, 'Fundamental Plan for National Resilience - For Building a Strong and Flexible Country-', 2018. [Accessed: Mar. 06, 2024], Available: https://www.cas.go.jp/jp/seisaku/kokudo_kyoujinka/en/fundamental_plan.pdf.
10. Ehime Prefecture, 'Agricultural Infrastructure Improvement and Rural Development in EHIME', 2023 (in Japanese). [Accessed: Feb. 06, 2024], Available: https://www.pref.ehime.jp/h35400/20/documents/08zentai-1.pdf.
11. Cabinet Office, Government of Japan, 'White Paper Disaster Management in Japan', 2019. [Accessed: Mar. 09, 2024], Available: https://www.bousai.go.jp/kaigirep/hakusho/pdf/R1_hakusho_english.pdf.
12. A. Shimpo, K. Takemura, S. Wakamatsu, H. Togawa, Y. Mochizuki, M. Takekawa, S. Tanaka, K. Yamashita, S. Maeda, R. Kurora, H. Murai, N. Kitabatake, H. Tsuguti, H. Mukougawa, T. Iwasaki, R. Kawamura, M. Kimoto, I. Takeyabu, Y. N. Takayabu, Y. Tanimoto, T. Horooka, Y. Masumoto, M. Watanabe, K. Tsuboki, and H. Nakamura, 'Primary Factors behind the Heavy Rain Event of July 2018 and the Subsequent Heat Wave in Japan', SOLA, vol. 15A, pp. 13–18, 2019, https://doi.org/10.2151/sola.15A-003.
13. T. Izumi, E. Takeyama, Y. Sato, and N. Kobayashi, 'Damage to Agricultural Infrastructure in Ehime Prefecture Resulting from the Heavy Rain Event of July 2018: - Focusing on Damage to Orchard Fields and Irrigation Tanks -', Journal of Rainwater Catchment Systems, vol. 26, no. 2, pp. 15–25, 2021, https://doi.org/10.7132/jrcsa.26_2_15.
14. K. Okada, Y. Makihara, A. Shinpo, K. Nagata, M. Kunitsugu, and K. Saito, 'Soil Water Index (SWI)', Tenki, vol. 48, no. 5, pp. 349–356, 2001 (in Japanese), https://doi.org/10.5771/9780739160046-349.
15. S. Mori and K. Ono, 'Landslide disasters in Ehime Prefecture resulting from the July 2018 heavy rain event in Japan', Soils and Foundations, vol. 59, no. 6, pp. 2396–2409, Dec. 2019, https://doi.org/10.1016/j.sandf.2019.11.009.
16. Ministry of Land, Infrastructure, Transportation and Tourism, 'About the Situation of Damage due to Heavy Rain Event of July 2018 (52nd Report)', 2019 (in Japanese). [Accessed: Feb. 06, 2024], Available: https://www.mlit.go.jp/common/001268344.pdf.
17. T. Kimura, T. Wakatsuki, R. Yamada, and T. Iguchi, 'Characteristics of the Magnitude and Distribution of Landslides Induced by the Heavy Rain Event of July 2018 in the Southwestern Part of Ehime Prefecture, Japan', National Disaster Research Report, vol. 53, pp. 67–82, 2019 (in Japanese with English abstract), https://doi.org/10.24732/nied.00002157.
18. S. Ishiguro and K. Kawase, 'Overview of Flood and Slope Failure in Ehime Prefecture Due to the Heavy Rain Event of July 2018', Geographical Sciences, vol. 75, no. 3, pp. 127–135, 2020 (in Japanese), https://doi.org/10.20630/chirikagaku.75.3_127.
19. Uwajima City Office, 'Uwajima City Reconstruction Plan', Mar. 2019 (in Japanese). [Accessed: Feb. 06, 2024], Available: https://www.city.uwajima.ehime.jp/uploaded/attachment/22642.pdf.
20. Japan Meteorological Agency, Radar/Rain Gauge Analyzed Precipitation 2018, [DVD], Tokyo, Japan: Japan Meteorological Business Support Centre, 2018.

Paper submitted: 10.11.2024
Paper revised: 04.02.2025
Paper accepted: 21.02.2025